Understanding the Giant Enhancement of Exchange Interaction in Bi_{2}Se_{3}-EuS Heterostructures

Jeongwoo Kim, Kyoung-Whan Kim, Hui Wang, Jairo Sinova, and Ruqian Wu

Phys. Rev. Lett. **119**, 027201 — Published 13 July 2017

DOI: 10.1103/PhysRevLett.119.027201

Understanding the giant enhancement of exchange interaction in Bi_2Se_3-EuS heterostructures.

Jeongwoo Kim[1], Kyoung-Whan Kim[2], Hui Wang[1], Jairo Sinova[2,3], & Ruqian Wu[1,*]

[1]*Department of Physics and Astronomy, University of California, Irvine, California 92697, USA*

[2]*Institut für Physik, Johannes Gutenberg Universität Mainz, Mainz, 55128, Germany*

[3]*Institute of Physics, Academy of Sciences of the Czech Republic, Cukrovarnická 10, 162 53 Praha 6, Czech Republic*

Abstract

A recent experiment indicated that a ferromagnetic EuS film in contact with a topological insulator Bi_2Se_3 might show largely enhanced Curie temperature and perpendicular magnetic anisotropy [Nature **533**, 513 (2016)]. Through systematic density functional calculations, we demonstrate that in addition to the factor that Bi_2Se_3 has strong spin orbit coupling, the topological surface states are crucial to make these unusual behaviors robust as they hybridize with EuS states and extend rather far into the magnetic layers. The magnetic moments of Eu atoms are nevertheless not much enhanced, unlike what was reported in the experiment. Our results and model analyses provide useful insights for how these quantities are linked, and pave a way for the control of properties of magnetic films via contact with topological insulators.

PACS: 73.20.At, 71.15.Mb, 75.70.Cn

Email: wur@uci.edu

Introducing spin polarization in topological insulators (TIs) is a critical issue for the application of their peculiar topological surface states (TSSs) in the next generation spintronic devices [1-3]. The emergent quantum phenomena such as the topological magneto-electric effect [4], the quantum anomalous Hall effect [1], and the large spin-orbit torque [5, 6] have inspired interdisciplinary endeavors to investigate their underlying scientific principles and to explore innovative materials with nontrivial topological properties. The conventional approach that is currently used to magnetize and manipulate the TSSs is magnetic doping, with magnetic dopants such as Cr [7-10], Fe [11-15], and Mn [16, 17] substituting the cations in TIs. Although successful observation of the quantum anomalous Hall effect has been reported for Cr- or V-doped $(Bi,Sb)_2Te_3$ [18-20], further progress has nonetheless been impeded by various technical issues, mostly due to the uncontrollability of dopant distribution and magnetic ordering. The heterostructures of ferromagnetic insulators (FIs)-TIs appear to be promising alternatives to imprint magnetization in TSSs through the interfacial proximity effect while the structural perfectness can be largely maintained [21-26].

Among a variety of FI-TI combinations, EuS-Bi_2Se_3 has attracted intense interest owing to several unusual ferromagnetic behaviors produced by the interfacial effects [26-30]. At first, the magnetism may survive up to room temperature [27], even though the Curie temperature of pure EuS is only 17 K [31]. Second, in spite of in-plane magnetic anisotropy of the bulk EuS, out-of-plane magnetization was observed for EuS-Bi_2Se_3 [26, 27]. Furthermore, extraordinarily enhanced magnetic signal was detected within the outermost two quintuple layers (QLs) of Bi_2Se_3 [26, 27]. All these observations indicate strong interplay between the magnetization of EuS and nonlocal TSSs of Bi_2Se_3, possibly via its large spin-orbit coupling (SOC); a thorough theoretical understanding is certainly desired.

In this Letter, we report results of systematic first-principles calculations and model analyses for the magnetic ordering of EuS-Bi_2Se_3. In addition to providing answers for the puzzling observations for EuS-Bi_2Se_3, we show that the strong SOC of Bi_2Se_3 plays a crucial role in determining the exchange coupling and spin orientation of EuS. Our results suggest the possibility of having unusual magnetic behaviors in FI-TI heterostructures, and lead to the establishment of general rules for the search of magnetic topological materials.

Our density functional theory (DFT) calculations were performed with the projected augmented plane-wave method [32, 33] as implemented in the Vienna *ab initio* simulation

package (VASP) [34]. We constructed a slab model that consists of 5 QLs Bi_2Se_3, 4 layer (~1.2 nm) EuS and a 15 Å vacuum, with the surface S atoms passivated by hydrogen atoms. We adopted the generalized gradient approximation (GGA) for the description of exchange-correlation interaction among electrons [35], along with the van der Waals correction for a better description of the long-range dispersion force [36]. Eu *f*-orbitals were considered as valence electrons and their U and J values were set at 8 eV and 1 eV, respectively [29]. The trend of unusual magnetic behavior is qualitatively the same as that without employing the *GGA+U* scheme. The SOC was included in the self-consistent calculations. The energy cutoff for the plane-wave expansion was set at 300 eV. We adopted a 15×15×1 $\boldsymbol{k}$-point grid to sample the Brillouin zone. Atomic relaxation was carried out until the change of total energy became less than 0.01 meV. The spin wave calculations were performed based on the fully unconstrained noncollinear magnetic formalism as implemented in VASP.

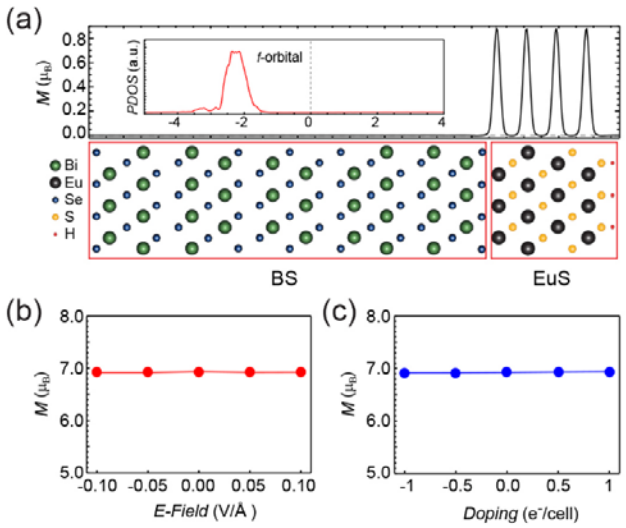

Figure 1 (Color online) (a) The local magnetization plot along the z-axis. The corresponding atomic structure of EuS-Bi_2Se_3 is shown in the bottom. Inset is the density of states for f-orbitals of Eu atoms. The variation of magnetization as function of (b) the electric field strength and (c) the doping level.

To understand the unusual magnetic behaviors of EuS-Bi_2Se_3, we first investigated the alteration of magnetization of EuS caused by the contact with TI. Out-of-plane magnetization is preferred in the optimized structure of EuS-Bi_2Se_3, in good agreement with experiment [26]. The spatial distribution of magnetization of Fig. 1(a) clearly shows that the spin magnetic moment is mostly localized at the Eu layers. Because the magnetization of EuS

originates from the heavily localized unpaired *f*-orbitals, the local spin magnetic moment of Eu (6.94 μ_B) is almost the same as that of the bulk EuS (6.92 μ_B). We note that the large enhancement of magnetic moment or the induced magnetic moment in TI was not found in our calculations, which is consistent with previous theoretical reports [30], but is contrary to experimental observations [26, 27]. To see if this discrepancy is due to simple artifacts, we also considered configurations that are terminated with S or Eu layer without H passivation as depicted in Fig. S1 in supplementary materials (SM). In all cases, the spin magnetic moments of Eu remain close to 7 μ_B and the orbital magnetic moment is, at the largest, 0.3 μ_B in the S-terminated structure. Therefore, we can conclude that the magnetic moment of Eu atom is well preserved in EuS-Bi_2Se_3 without any indication of strong enhancement. Furthermore, magnetic moment of Eu is stable against various external perturbations such as electric fields and electron (or hole) doping [Figs. 1(b) and (c)], because the *f*-orbitals lie far below the Fermi level [Fig. 1(a), inset]. For example, the magnetic moment of Eu is almost fixed around 7 μ_B in a wide range of electric fields (-0.1 to 0.1 V/Å). Even when we shift the Fermi level to mimic the variation of electron population, Eu atoms still have almost the same magnetic moment because the states near the Fermi level, mostly the *p*- or *d*-orbitals, are not the origin of the spin polarization around Eu.

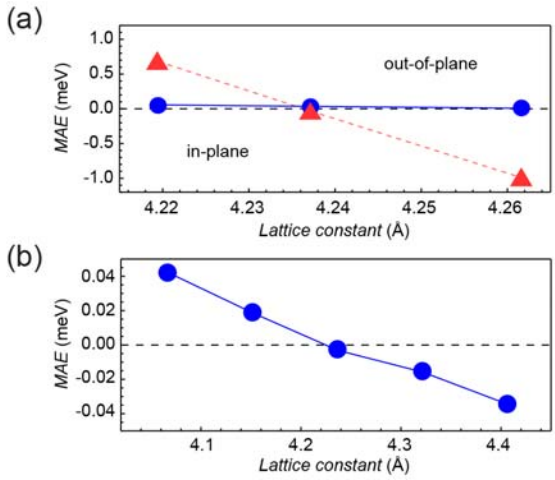

Figure 2 (Color online) (a) Calculated magnetic anisotropy energy (MAE) of EuS-Bi_2Se_3 for varying the lattice constant. The SOC constants of Bi and Se are changed to zero (blue dots) from native values (red triangles). (b) Calculated magnetic anisotropy energy of EuS as a function of the lateral lattice constant in the bulk EuS.

Now we address the effect of the TSSs of Bi_2Se_3 on the magnetic anisotropy energy (MAE) of EuS, which has rarely been studied. It is intriguing that the contact with TI may cause a spin reorientation in EuS-Bi_2Se_3. As shown in Fig. 2, EuS-Bi_2Se_3 has a strong magnetostriction, as attested by the steep change of MAE against the change of lateral lattice constant. In the optimized structure (a=4.22 Å), EuS-Bi_2Se_3 has the positive MAE (0.65 meV/Eu), which means the magnetization is pointing along the surface normal [Fig. 2(a)] as observed in experiment. In contrast, the relaxed bulk EuS (a=4.24 Å) has an in-plane easy axis [Fig. 2(b)]. Although the smaller lattice constant of Bi_2Se_3 (a=4.19 Å) versus that of EuS (a=4.24 Å) appears to be the driving force for the spin reorientation, the MAE of EuS-Bi_2Se_3 is about a hundred times larger than that of EuS in the same range of strain. Such a strong enhancement in MAE is rather unusual and deserves a careful analysis. Since Bi_2Se_3 remains nonmagnetic in EuS-Bi_2Se_3 as displayed in Fig. 1(a), the large MAE should be attributed to the effect of peculiar surface state of TI. To prove this, we tuned the strength of SOC of Bi_2Se_3 to zero and found that MAE of EuS-Bi_2Se_3 becomes two orders smaller, comparable to that of pure EuS, in the entire range of lattice strain [Fig. 2(a)]. Our findings unambiguously point out the importance of the strong SOC inherent in the topologically nontrivial surface states of TIs in determining the spin orientation of thin magnetic films. As the thickness of EuS film increases, it is perceivable that the proximity effect of Bi_2Se_3 layers decays so the easy axis gradually turns to in-plane due to the shape anisotropy, as observed in experiment [26, 27].

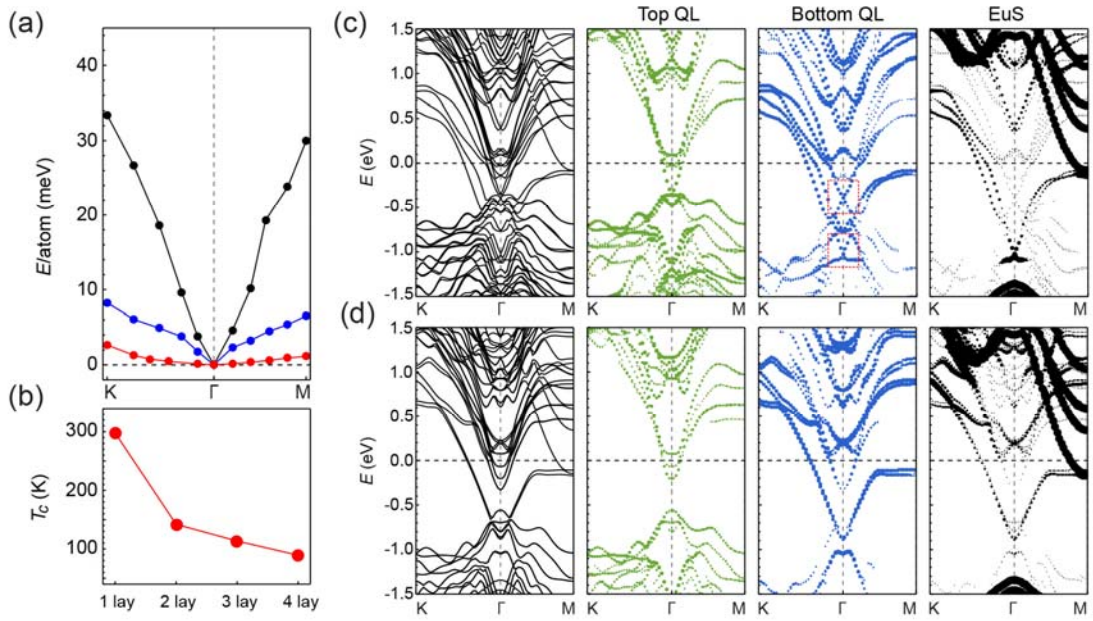

Figure 3 (Color online) (a) Calculated magnon dispersion relations of 4-layer EuS film on Bi_2Se_3 and the bulk EuS (red). The SOC constants of Bi and Se are changed to zero (blue) from native values (black). (b) The variation of Curie temperature of EuS-Bi_2Se_3 with the thickness of EuS. Calculated band structures of EuS-Bi_2Se_3 (c) with and (d) without the SOC of Bi_2Se_3. The contributions of top (surface plane) QL, bottom (interface plane) QL, and EuS layers are represented in green (left), blue (middle), and black (right) respectively.

Another intriguing experimental finding in EuS-Bi_2Se is its surprisingly high Curie temperature. This indicates the strong enhancement of exchange interactions among Eu atoms due to the additional coupling channel via the TSSs at the interface. A direct approach for the determination of exchange constant (J) is through calculation of spin wave spectrum in the momentum space. The spin wave excitation can be appropriately described in the primitive unit cell by applying the generalized Bloch's theorem for the spin spiral structures [38]. The exchange constants can be extracted from the magnon dispersion for the classical Heisenberg model. As shown in Fig. 3(a), the excitation energy at the K point is less than 3 meV for the bulk EuS (red) but it drastically increases up to 33.4 meV when EuS layers are in contact with Bi_2Se_3 (black, also see the effect of U in Fig. S2 in SM). It clearly suggests that the ferromagnetic exchange is enhanced by the presence of Bi_2Se_3 layers. Using the mean-field approximation, we estimated the Curie temperature from the calculated magnon dispersion, in order to compare with experiment. Fig. 3(b) shows that the Curie temperature may reach up to 300 K for a monolayer EuS on Bi_2Se_3. Although the estimated Curie temperature steadily decreases as the thickness of the EuS film becomes larger (see Fig. S3 in SM for the thickness dependence of J), it is still substantially higher than that of the bulk EuS of 17 K. Obviously, the TSSs have dual effects on both the magnetic anisotropy and magnetic ordering of EuS, and these effects may find important use for the manipulation of magnetic materials.

To shed lights on the fundamental aspects of the proximity effect of TSSs on magnetic films, we tune the SOC constant of the Bi_2Se_3 layer and observe the consequence. When the SOC is set to zero [blue line in Fig. 3(a)], the energy of the spin wave at the zone boundary is drastically reduced to less than 10 meV. We also observe that the slope of the magnon dispersion is very sensitive to the SOC strength under its continuous variation (see Fig. S4 in SM). Moreover, we calculated the band structure of EuS-Bi_2Se_3 heterostructure for different values of SOC in Bi_2Se_3. For the case with full SOC strengths, band structures in Fig. 3(c) show that the TSS is mostly localized in the top QL (surface plane) in the side of

vacuum, in spite of a slight increase of the in-plane lattice constant. Due to the potential difference between EuS and Bi_2Se_3 and hence the charge redistribution at the interface (see Fig. S5 in SM), the band bending occurs and two linear Dirac cones (red dotted boxes) with the same spin helicity can be seen [29, 30]. The X-shape band around -0.3 eV in the vicinity of the Γ point (high-energy TSS) results from the rehybridization between TSS and quantum-well states of Bi_2Se_3 (Fig. S6 in SM), which frequently appears in TI heterostructures [25, 39, 40]. This Dirac state localizes mostly in the second QL from the interface [30] and quickly merges into the bulk bands away from the Brillouin zone center. On the contrary, the Dirac state near -1.0 eV extends rather far into the EuS layers as indicated by its heavy weight in the right panel of Fig. 3(c) and the characteristic in-plane spin helicity is still maintained. Fig. 3(c) also shows Rashba bands near -0.2 eV around the Γ-point, but they have negligible weights in the EuS layers and hence should not play an important role in affecting magnetic ordering and magnetic anisotropy of EuS.

In Fig. 3(d), one may note that the absence of SOC makes substantial changes in the electronic structures of EuS-Bi_2Se_3. Without the topological protection, electrons states of the top and bottom QLs are very different and the intermix between states in EuS and Bi_2Se_3 sides are much reduced. While the top QL has a trivial band gap, the interface QL is metallic and the weights of Bi_2Se_3 states in EuS become small below the Fermi level. Obviously, the most remarkable change caused by the adjustment of SOC is the disappearance of the TSS of Bi_2Se_3, and the reduction of the spatial range of the Bi_2Se_3 in EuS. Indeed, if we place EuS on PbSe and Pb, materials that have large SOC but are topologically trivial, the magnon energy is much smaller than that on Bi_2Se_3 (see Fig. S7 in SM). This analysis again implies a link between the existence of TSSs of Bi_2Se_3 and the extraordinary magnetic properties of the EuS-Bi_2Se_3 interface. The changes of MAE and J of EuS-Bi_2Se_3 result not only from the SOC alone, but also from the large spatial extension as provided by the new interfacial Dirac states. We want to point out that the magnetic moment of interfacial Eu atom remains almost unchanged (6.93 μ_B) when the SOC of Bi_2Se_3 is tuned.

As illustrated in Fig. 4(a), *f*-orbitals of Eu atoms mainly overlap and hybridize with valence bands below the Fermi level, and hence the effect of states near the Fermi level on the exchange interaction should be weak in ordinary cases, as exemplified in EuS-Pb in Fig. S7 (b). However, the conduction and valence bands of TIs are interconnected and the Dirac states of Bi_2Se_3 contribute to the magnetic properties EuS in a large energy range. In addition,

the highly coherent TSSs may mediate exchange coupling between Eu atoms through the Ruderman-Kittel-Kasuya-Yosida (RKKY) type interactions. Figure 4(b) demonstrates that the exchange constant is very sensitive to the position of the Fermi level, and may change sign when it sweeps across the Dirac point, which is a characteristic of the RKKY-type interaction. Since the position of Fermi level can be conveniently controlled via back gates, this provides a handy way to control the Curie temperature of EuS-Bi_2Se_3.

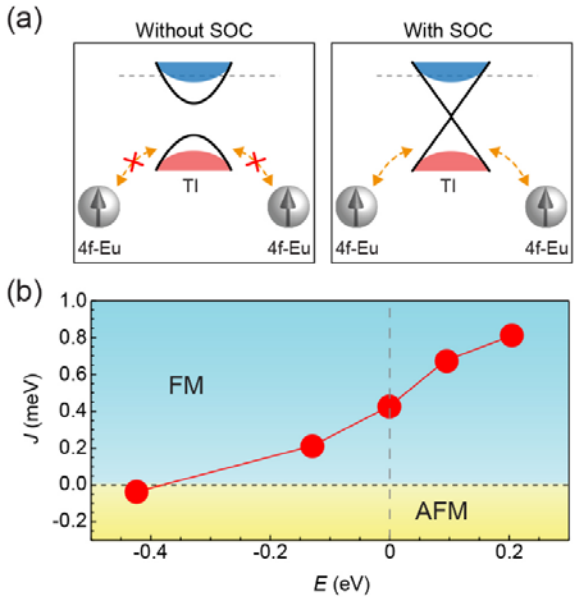

Figure 4 (Color online) (a) Schematic drawings for TSS-mediated FM ordering between Eu atoms. The FM ordering of localized spins (gray arrows) mediated by TSSs (black lines) is weakened by the absence of the SOC effect of Bi_2Se_3. (b) The variation of the exchange constant (J) of EuS-Bi_2Se_3 with the Fermi level; positive (negative) if FM (AFM) is ground magnetic state.

To gain qualitative insights on the emergence of out-of-plane magnetic anisotropy mediated by TSS and its correlation with the exchange interaction, we construct a simple model Hamiltonian for EuS/TI as $H = H_{\mathrm{TSS}} + H_{\mathrm{EuS}}(\mathbf{m}) + H_{\mathrm{int}}$. This model consists of contributions from TSS (H_{TSS}), local magnetic moment in EuS (H_{EuS}), and their interaction (H_{int}). H_{TSS} is modeled by linear dispersive bands with a Dirac cone $H_{\mathrm{TSS}} = \hbar v_F \boldsymbol{\sigma} \cdot (\mathbf{k} \times \hat{\mathbf{z}})$ [41] where v_F is the Fermi velocity, $\mathbf{k}$ is the in-plane momentum of electrons in TSS, $\boldsymbol{\sigma}$ is the spin Pauli matrix for electrons in TSS, and $\hat{\mathbf{z}}$ is the interface normal direction. $H_{\mathrm{EuS}} = H_{\mathrm{EuS}}(\mathbf{m})$ is the energy functional of the magnetization direction $\mathbf{m}$ and determines

intrinsic properties of EuS. Lastly, H_{int} is set to be equal to $u\boldsymbol{\sigma}\cdot\mathbf{m}$ which describes an exchange-type interaction between TSS and the local magnetic moment with the characteristic energy u. We omit the non-topological Rashba term as it does not necessarily lead to out-of-plane magnetic anisotropy [42].

By integrating out the degrees of freedom of the TSS as described in SM, we obtain a reduced Hamiltonian $H_{\mathrm{reduced}} = H_{\mathrm{TSS}}^{\mathrm{eff}}(\mathbf{m}) + H_{\mathrm{EuS}}(\mathbf{m})$. Following the procedure for the calculation of MAE emerging from Rashba SOC and exchange interaction with magnetization [42], the effective Hamiltonian from TSS can be finalized to $H_{\mathrm{TSS}}^{\mathrm{eff}}(\mathbf{m}) = -Au^2m_z^2$, where A is a positive proportionality constant. Our result shows that the total energy is reduced when the local magnetic moments in EuS point toward $\hat{\mathbf{z}}$, implying the emergence of out-of-plane magnetic anisotropy mediated by TSS as found in DFT calculations and observed in experiment [26].

The model can be simply extended to include the coupling between TSS and multiple magnetic moments as $H_{\mathrm{int}} = \sum_i u_i\boldsymbol{\sigma}\cdot\mathbf{m}_i$ where i is the index of the magnetic moment. The same formalism results in $H_{\mathrm{TSS}}^{\mathrm{eff}}(\mathbf{m}) = -A\sum_i u_i^2m_{iz}^2 - 2A\sum_{i\neq j} u_iu_jm_{iz}m_{jz}$ where the two terms describe the emergent magnetic anisotropy and exchange interaction, respectively. For the simplest case $u_i = u$, an additional exchange energy $2Au^2$ arises in the same order of the anisotropy energy, consistent with our DFT calculations. In addition, this model also gives a correct Fermi level dependence of MAE (Fig. S8), indicating that it captures the main issue: the important role of TSS in governing properties of magnetic thin films in contact with TIs. Of course, this simple model has no details of the intricate band structures and is not designed for making quantitative predictions.

In summary, we showed that the proximity effect of topological surface states of Bi_2Se_3 may strongly enhance magnetic ordering and lead to out-of-plane magnetic anisotropy of EuS thin film. The large exchange coupling in the Eu layer is mediated by the Dirac states via the RKKY-type mechanism and the Curie temperature may persist up to 300 K. Our results provide the keys for understanding magnetism at interfaces with topological insulators and lay a foundation for the design of spintronic devices.

This work was support by the SHINES, an Energy Frontier Research Center founded by the U. S. Department of Energy, Office of Science, Basic Energy Science under Award

SC0012670. Calculations were performed on parallel computers at NERSC supercomputer centers. J.S. and K.W.K. acknowledge the support of the Alexander von Humboldt Foundation, the ERC Synergy Grant SC2 (No. 610115), and the Transregional Collaborative Research Center (SFB/TRR) 173 SPIN+X. K.W.K also acknowledges support by Basic Science Research Program through the National Research Foundation of Korea (NRF) funded by the Ministry of Education (2016R1A6A3A03008831),

References

[1] R. Yu, W. Zhang, H.-J. Zhang, S.-C. Zhang, X. Dai, and Z. Fang, Science **329**, 61 (2010).

[2] G. J. Ferreira, and D. Loss, Phys. Rev. Lett. **111**, 106802 (2013).

[3] R. Li, J. Wang, X.-L. Qi, and S.-C. Zhang, Nat. Phys. **6**, 284 (2010).

[4] A. M. Essin, J. E. Moore, and D. Vanderbilt, Phys. Rev. Lett. **102**, 146805 (2009).

[5] Y. Fan *et al.*, Nat. Nanotech. **11**, 352 (2016).

[6] Y. Fan *et al.*, Nat. Mater. **13**, 699 (2014).

[7] M. Liu *et al.*, Phys. Rev. Lett. **108**, 036805 (2012).

[8] J.-M. Zhang, W. Zhu, Y. Zhang, D. Xiao, and Y. Yao, Phys. Rev. Lett. **109**, 266405 (2012).

[9] X. Kou *et al.*, ACS Nano **7**, 9205 (2013).

[10] J. Kim, S.-H. Jhi, and R. Wu, Nano Lett. **16**, 6656 (2016).

[11] Y. L. Chen *et al.*, Science **329**, 659 (2010).

[12] Y. Okada *et al.*, Phys. Rev. Lett. **106**, 206805 (2011).

[13] L. A. Wray, S.-Y. Xu, Y. Xia, D. Hsieh, A. V. Fedorov, Y. S. Hor, R. J. Cava, A. Bansil, H. Lin, and M. Z. Hasan, Nat. Phys. **7**, 32 (2011).

[14] J. Kim, and S.-H. Jhi, Phys. Rev. B **92**, 104405 (2015).

[15] J. Honolka *et al.*, Phys. Rev. Lett. **108**, 256811 (2012).

[16] Y. S. Hor *et al.*, Phys. Rev. B **81**, 195203 (2010).

[17] J. Henk, M. Flieger, I. V. Maznichenko, I. Mertig, A. Ernst, S. V. Eremeev, and E. V. Chulkov, Phys. Rev. Lett. **109**, 076801 (2012).

[18] C.-Z. Chang *et al.*, Science **340**, 167 (2013).

[19] C.-Z. Chang, W. Zhao, D. Y. Kim, H. Zhang, B. A. Assaf, D. Heiman, S.-C. Zhang, C.

Liu, M. H. W. Chan, and J. S. Moodera, Nat. Mater. **14**, 473 (2015).

[20] J. G. Checkelsky, R. Yoshimi, A. Tsukazaki, K. S. Takahashi, Y. Kozuka, J. Falson, M. Kawasaki, and Y. Tokura, Nat. Phys. **10**, 731 (2014).

[21] I. Garate, and M. Franz, Phys. Rev. Lett. **104**, 146802 (2010).

[22] M. Lang *et al.*, Nano Lett. **14**, 3459 (2014).

[23] M. Li *et al.*, Phys. Rev. Lett. **115**, 087201 (2015).

[24] W. Liu *et al.*, Nano Lett. **15**, 764 (2015).

[25] S. V. Eremeev, V. N. Men'shov, V. V. Tugushev, P. M. Echenique, and E. V. Chulkov, Phys. Rev. B **88**, 144430 (2013).

[26] P. Wei, F. Katmis, B. A. Assaf, H. Steinberg, P. Jarillo-Herrero, D. Heiman, and J. S. Moodera, Phys. Rev. Lett. **110**, 186807 (2013).

[27] F. Katmis *et al.*, Nature **533**, 513 (2016).

[28] Q. I. Yang *et al.*, Phys. Rev. B **88**, 081407 (2013).

[29] A. T. Lee, M. J. Han, and K. Park, Phys. Rev. B **90**, 155103 (2014).

[30] S. V. Eremeev, V. N. Men′shov, V. V. Tugushev, and E. V. Chulkov, J. Magn. Magn. Mater. **383**, 30 (2015).

[31] P. Schwob, and O. Vogt, Phys. Lett. A **24**, 242 (1967).

[32] P. E. Blöchl, Phys. Rev. B **50**, 17953 (1994).

[33] G. Kresse, and D. Joubert, Phys. Rev. B **59**, 1758 (1999).

[34] G. Kresse, and J. Hafner, Phys. Rev. B **47**, 558 (1993).

[35] J. P. Perdew, K. Burke, and M. Ernzerhof, Phys. Rev. Lett. **77**, 3865 (1996).

[36] S. Grimme, J. Antony, S. Ehrlich, and H. Krieg, J. Chem. Phys. **132**, 154104 (2010).

[37] D. Hobbs, G. Kresse, and J. Hafner, Phys. Rev. B **62**, 11556 (2000).

[38] L. M. Sandratskii, Adv. Phys. **47**, 91 (1998).

[39] K.-H. Jin, H. W. Yeom, and S.-H. Jhi, Phys. Rev. B **93**, 075308 (2016).

[40] V. N. Men'shov, V. V. Tugushev, S. V. Eremeev, P. M. Echenique, and E. V. Chulkov, Phys. Rev. B **88**, 224401 (2013).

[41] L. Fu, Phys. Rev. Lett. **103**, 266801 (2009).

[42] K.-W. Kim, K.-J. Lee, H.-W. Lee, and M. D. Stiles, Phys. Rev. B **94**, 184402 (2016).